Light Collection Uniformity of Lead Tungstate Crystals for the CMS Electromagnetic Calorimeter

D. Britton, M. Ryan, X. Qu [1]

Imperial College, London

Abstract

A technique has been developed to measure the light collection uniformity of lead tungstate crystals for the CMS electromagnetic calorimeter. The use of a hybrid photomultiplier tube allows a precision measurement despite the intrinsically low light yield. It is found that shading the chamfered edges of the crystals with a pencil can achieve a reduction in the front-non uniformity of approximately 0.1 $\%/X_0$. Similar effects are observed by de-polishing the chamfers.

Key words: CMS, Calorimeter, Lead Tungstate, HPMT
PACS:

1 Introduction

The electromagnetic calorimeter (ECAL) [1] of the CMS detector is intended to play a key role in the discovery and measurement of the Higgs boson and in the identification of signatures of new physics beyond the Standard Model at the LHC. The ECAL will consist of about 75000 scintillating lead tungstate ($PbWO_4$) crystals arranged in a barrel section and two endcap sections. Stringent demands are placed upon the ECAL performance in order to measure as accurately as possible the energies of electrons and photons. The energy resolution is parameterised as follows:

$$\frac{\sigma}{E} = \frac{a}{\sqrt{E}} \oplus \frac{b}{E} \oplus c \tag{1}$$

[1] Now at Applied Scintillation Technologies Ltd., Harlow, CM19 5BZ, UK.

where a is a stochastic term, b the electronics noise term and c is a constant term. Calorimeters employing fully active media can usually achieve very good stochastic terms; the energy resolution, particularly at high energy, is then dominated by the constant term.

Most pertinent to the work presented in this paper is the contribution to the constant term from non-uniformity in light collection. When a high energy particle is incident upon a scintillating crystal, an EM shower develops with the secondary shower particles exciting scintillation in the material. The largest energy deposit occurs in the shower maximum region, typically within the first 4-12 X_0. For a given incident particle energy, the depth of the maximum energy deposit fluctuates from shower to shower and any property of the crystal which creates a dependency of the amount of light collected on its position of origin will therefore introduce a contribution to the energy resolution.

The CMS ECAL crystals are tapered in shape to obtain a pseudo-pointing geometry. This shape focuses light produced at the small, tapered end of the crystal onto the photodetector mounted at the rear, thereby increasing its chances of being detected when compared with light produced further along the crystal. Competing with this effect is the light attenuation length, which decreases the probability of detecting light produced further away from the photodetector. Although these effects approximately cancelled in early crystals, current production-quality crystals have attenuation lengths of several metres, giving a non-uniform light response (illustrated schematically in Figure 1). Simulation studies have shown that in order to achieve the design performance target of a 0.3% contribution to the constant term from residual longitudinal non-uniformity the tolerable change in detected light is 0.35 $\%/X_0$ [2].

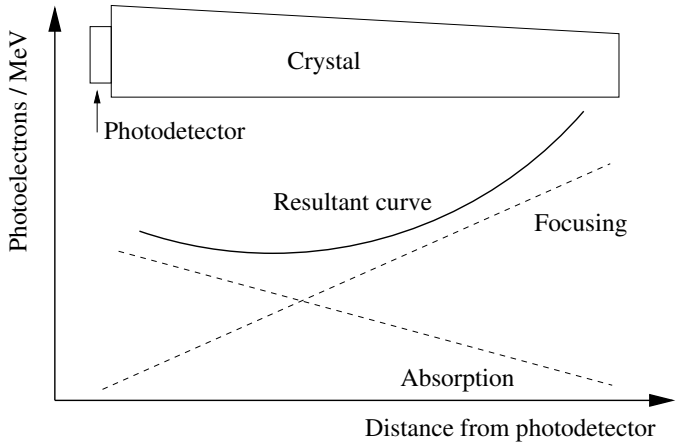

Fig. 1. Schematic of light collection uniformity curve. The focusing and absorption lines illustrate the influence that these effects have on the light yield as a function of distance from the photodetector and the part they play in determining the overall light collection curve.

For barrel crystals, the solution adopted for achieving the desired uniformity was to depolish one face of each crystal to randomise the angle of reflection [3]. This reduces the light collection dependency on position along the crystal but requires the crystal to be surrounded by a reflective layer to recover light that escapes through the roughened surface. In the endcaps, the crystals are 60% larger and the taper is less significant which reduces the focusing effect. It is hoped that the final production-quality endcap crystals will not require the additional step of depolishing to achieve the required uniformity. This would also avoid the need to identify a reflective layer that is sufficiently radiation-hard to withstand the intense fields in the end-cap regions. The reduction in the inactive material between crystals is also beneficial.

In this paper we present our studies of endcap crystal uniformity using a hybrid photomultiplier tube. The experimental setup and its performance are described. The effects that the crystal surroundings have on uniformity are investigated and the results compared with CERN ACCOS [4] data for the same crystals. Techniques for improving the uniformity of endcap crystals are presented.

2 Experimental Techniques

The crystal measuring apparatus shown schematically in Figure 2 is based on a DEP [2] hybrid photomultiplier tube (HPMT) capable of detecting individual photons with excellent resolution (we observe a FWHM of 16% on the first photoelectron peak). As shown in Figure 3(a), the first 18 photoelectron peaks can be discerned before backscattering of the photoelectrons from the diode completely washes out the peaks.

The HPMT used has a 40 mm diameter quartz window and a S20UV photocathode with a quantum efficiency of 23% at 425 nm. Photoelectrons released from the photocathode are accelerated through a 15 kV potential, generated by a purpose-built low noise power supply, toward a silicon diode. The diode is biased at 60 V to collect the charge generated. Signals collected by the diode are first amplified by the built-in preamplifier before being passed to an ORTEC 672 amplifier, set at a gain of 100 with a shaping time of 0.5 μs. The signals are then relayed to an ORTEC multi-channel buffer PC card for digitisation. The data are acquired from the card using the program MAESTRO in conjunction with a LabVIEW virtual instrument.

Scintillation in a crystal is stimulated by γ-rays from a ^{60}Co source, custom-ordered with a low activity of 20 kBq to reduce the effects of pile-up. The

[2] Delft Instruments, the Netherlands.

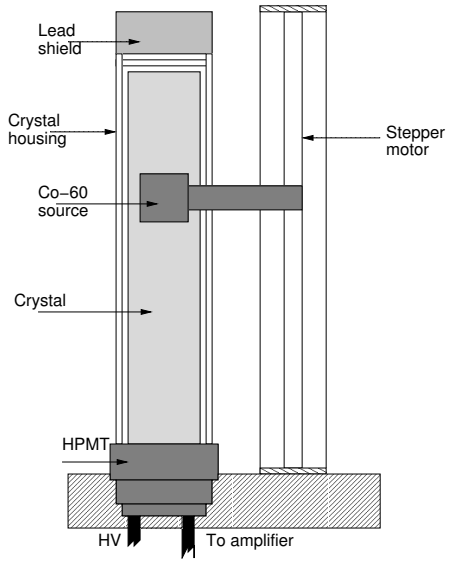

Fig. 2. Schematic diagram of HPMT setup.

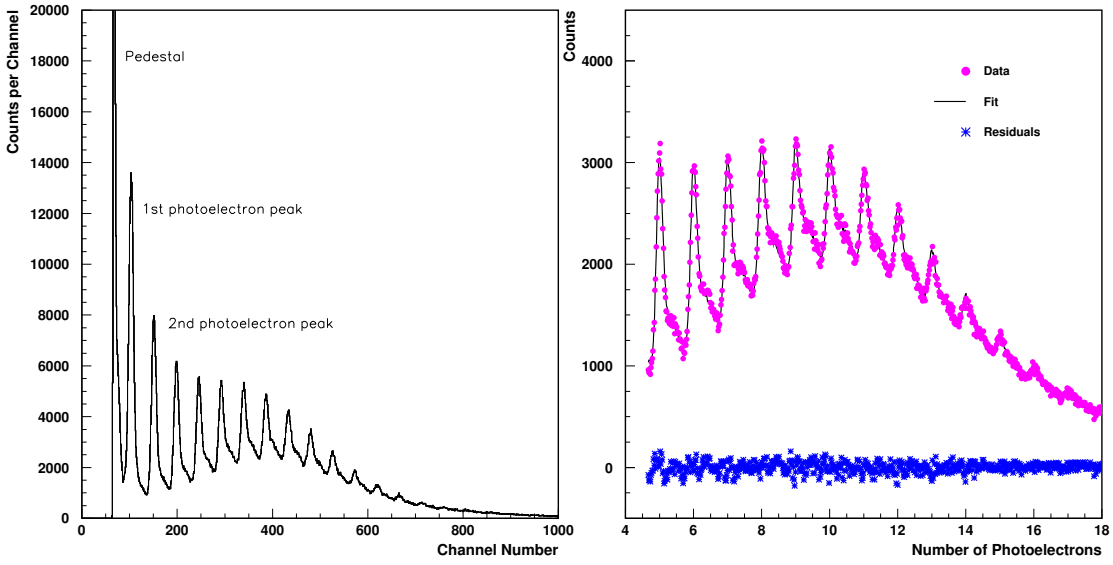

(a) Photoelectron spectrum obtained with a HPMT.

(b) A fitted spectrum.

Fig. 3. HPMT spectra.

point source is mounted on a linear stage to enable positioning of the source anywhere along the crystal's length, up to 195 mm from the small (tapered) end. The stage is controlled by a digital positioning system (DPS). Commands may be sent to the DPS from the PC using LabVIEW software and a GPIB interface card. The apparatus is housed within a light tight box; temperature in the box is stabilised at 18±0.1°C (the nominal operating temperature of

the ECAL) by a closed-circuit water cooling system.

3 Uniformity Measurements

3.1 Procedure

A uniformity measurement consists of measuring the average light yield at 19 points along the length of a crystal in a period of about 1.5 hours. The crystal is first cleaned to ensure there are no fingerprints or other deposits on the surface. The HPMT is mounted such that it can be rotated into the horizontal position so that the crystal, with optical grease applied to the rear face, can be gently slid up against the HPMT window. The crystal is supported by the copper housing and the entire assembly is then rotated to the vertical position. This procedure reduces the risk of damage to the HPMT window and helps ensure a reproducible coupling between the crystal and detector. A lead shield is placed on top of the crystal housing to enable 'no-source' background spectra to be recorded when the source is raised above the top of the crystal.

A full scan consisted of an initial and final spectrum acquired with the source shielded from the crystal. In between, 19 spectra were acquired each with a 4 minute integration period, with the source positioned at 10 mm intervals along the crystal length (starting at 15 mm from the small end). The diode bias was set at 60 V and the dark current allowed to stabilise for 20 minutes after the high voltage was ramped to 15 kV at the start of the scan.

3.2 Data Fitting

To obtain a quantitative measure of the light collection non-uniformity, the average light yield is extracted from each of the spectra using a detailed fitting function developed [5] from first principles. The 1.2 and 1.3 MeV γ-rays from the ^{60}Co source are prone to Compton scattering leading to a wide, but calculable, distribution of deposited energy. This must be convoluted with a Poisson distribution due to the low number of photoelectrons produced, which gives rise to the set of individual photoelectron peaks observed. Occasionally, however, the photoelectrons backscatter from the diode depositing only a fraction of their energy and this gives rise to the shoulders seen on the peaks in Figure 3. For each photopeak, all the possible combinations of one or more backscatterings have to be considered and this effect explains both the continuum under the peaks and limit on the number of peaks that can be resolved.

3.2.1 Front Non-Uniformity and Rear Non-Uniformity

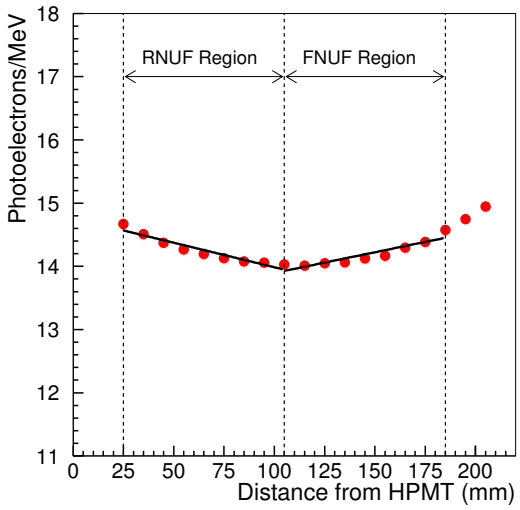

Fig. 4. A typical light yield uniformity curve.

After a uniformity scan has been performed and the data fitted to extract the average number of photoelectrons per MeV of energy deposited in the crystal, the non-uniformity is quantified by plotting this average against the position of the source from the HPMT as shown in Figure 4.

A straight line fit is performed to the data in two regions. The most important of these is in the shower maximum region, between 105 mm and 185 mm from the HPMT (3 X_0 - 10 X_0 from the small end). This the Front Non-Uniformity region (FNUF) and it is the value of the FNUF upon which the limit of 0.35 $\%/X_0$ is placed. A similar fit is performed on the data in the region 25 mm to 105 mm from the HPMT and the value of the non-uniformity in this region is called the Rear Non-Uniformity (RNUF). The FNUF and RNUF are calculated using the following equation [6]:

$$NUF(\%/X_0) = \frac{m}{(11.5m + c)} \times X_0^{PWO} \times 100 \qquad (2)$$

where m is the gradient, c the intercept from the linear fit and X_0^{PWO} is the radiation length of lead tungstate (0.89 cm).

3.3 Precision and Reproducibility

Initial estimates of the measurement errors were made by repeatedly measuring the FNUF of a single unwrapped crystal. For each measurement the crystal

was cleaned and remounted on the HPMT. This method not only includes the error from the HPMT but also the fitting errors. The results are summarised in Figure 5.

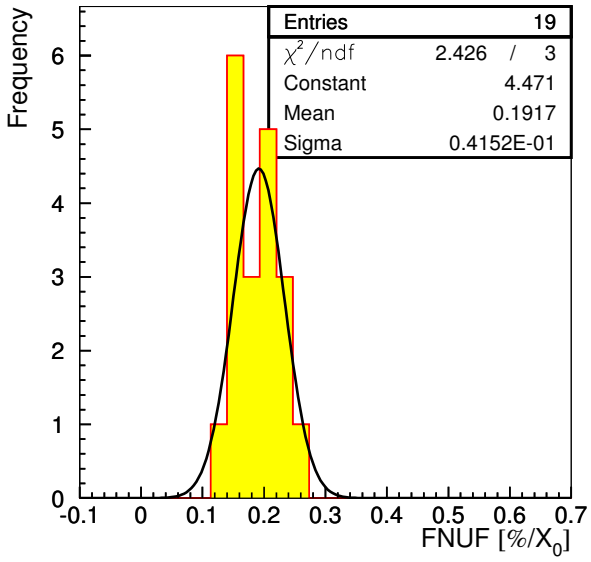

Fig. 5. Distribution of FNUFs measured repeatedly for a single crystal.

Performing a Gaussian fit to this data gives a sigma of about 0.04 $\%/X_0$. An alternative method of estimating the experimental error comes from correlations between different measurements using the equipment. From the correlations between wrapped and unwrapped crystals, and unwrapped crystals and crystals measured in the alveolar (Figure 7 in Section 4.3) we estimate an error of 0.05 $\%/X_0$. We adopt this latter number as the experimental resolution of our data.

4 Uniformity Studies of Pre-production Crystals

4.1 Crystal Samples

A sample of 20 crystals from the 2001 endcap pre-production batch from Bogoroditsk Techno Chemical Plant (BTCP) in Russia were delivered to Imperial College after evaluation at CERN. In April 2003 a further 32 crystals from this batch were received. Details of initial tests on these crystals performed at CERN may be found in reference [7]. Several of the samples received are 'anomalous' FNUF crystals; they have abnormally large values of FNUF.

4.2 Crystal Measurements

The first consignment of 20 crystals have been measured in three different configurations; namely unwrapped, wrapped in tyvek and contained within a carbon fibre alveolar support structure identical to the final endcap design. Alveolar measurements have also been performed on the second consignment of 32 crystals (one crystal could not be fitted due to low light yield).

- **Unwrapped** - in this configuration, crystals have no wrappings except the crystal housing structure and a piece of tyvek on the front face. This means that three of the crystal faces are separated by a small air gap from the copper surfaces of the apparatus.
- **Tyvek Wrapping** - tyvek is a polyethylene fibre product, manufactured by DuPont, which has good reflective properties. A tyvek envelope was modified to wrap a crystal, leaving only the photodetector face exposed.
- **Alveolar Container** - in the final detector configuration, the endcap crystals will be arranged in 5×5 arrays called *supercrystals*. Supercrystals are housed in a carbon fibre structure known as an *alveolar*. A prototype alveolar was adapted to house one crystal (including tyvek on the front face) within the HPMT configuration. This has allowed investigations into the effect of this structure on endcap uniformity.

Data for these measurements are presented in Figure 6 and in Table 1. The results are discussed in Section 4.3.

4.3 Effects of Crystal Surroundings on Uniformity

It can be seen from the data and Figure 7 that the wrapping of endcap crystals has a noticeable effect on the FNUF. Wrapped crystals exhibit a systematically higher FNUF than either unwrapped crystals or crystals in the alveolar. The average FNUF for wrapped crystals was 0.5 $\%/X_0$, which is 0.22 $\%/X_0$ greater than the average for unwrapped crystals and 0.11 $\%/X_0$ greater than for crystals measured in the alveolar.

As expected, highest light yields were obtained when using the tyvek wrapping, with an average of 11.2 photoelectrons/MeV. When using the alveolar an average light yield of 8.5 photoelectrons/MeV is observed, a reduction of about 24% compared to the wrapped case.

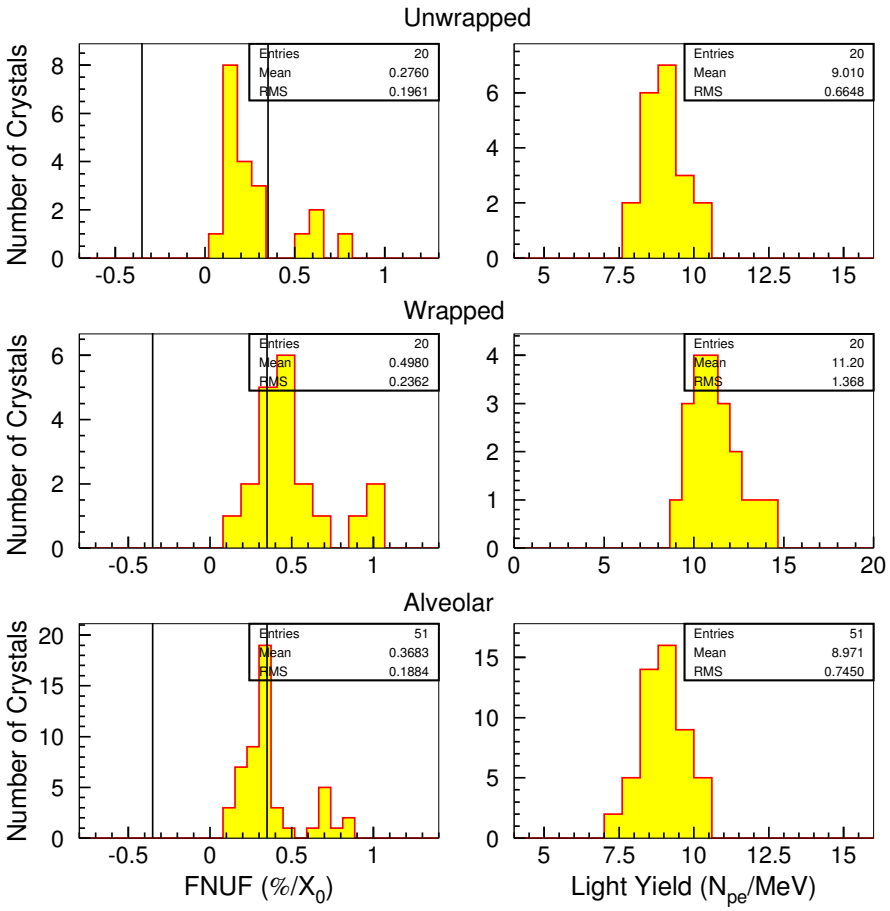

Fig. 6. Histograms of FNUF and light yield for crystals measured in 3 different surroundings. The vertical lines in the plots on the left hand side delineate the FNUF limits of $\pm 0.35\%/X_0$.

5 Comparison with CERN ACCOS Data

Before assembly of the ECAL, various parameters will be measured for each crystal, such as their dimensions, optical transmission, light yield and non-uniformity. To measure such a large number of crystals using standard laboratory equipment is unfeasible.

At CERN, an automatic crystal quality monitoring system (ACCOS) has been developed to measure large numbers of crystals in as short a time as possible [4]. As far as light yield measurements are concerned, it is noted from reference [4] that crystals are not optically coupled to the PMT and are unwrapped during this procedure. The decay time spectrum of the scintillation light is measured at 21 points along the length of each crystal, using a ^{22}Na source which emits two 511 keV photons. The detection of the first photon in a BaF_2 crystal initiates the start of a measurement and the detection of the

	FNUF ($\%/X_0$)	RNUF ($\%/X_0$)	Light Yield (N_{pe}/MeV)
Unwrapped			
Average	0.28 ± 0.01	-0.31± 0.01	9.02 ± 0.02
Maximum	0.81 ± 0.05	0.02 ± 0.05	10.4 ± 0.1
Minimum	0.10 ± 0.05	-0.58 ± 0.05	8.1 ± 0.1
Wrapped			
Average	0.50 ± 0.01	-0.36 ± 0.01	11.21 ± 0.02
Maximum	0.99 ± 0.05	0.18 ± 0.05	14.1 ± 0.1
Minimum	0.15 ± 0.05	-0.69 ± 0.05	9.1± 0.1
Alveolar			
Average	0.39 ± 0.01	-0.03 ± 0.01	8.54 ± 0.02
Maximum	0.87 ± 0.05	0.46 ±0.05	10.4 ± 0.1
Minimum	0.19 ± 0.05	-0.61 ± 0.05	7.4 ± 0.1

Table 1
Data for the 20 crystals measured in 3 configurations.

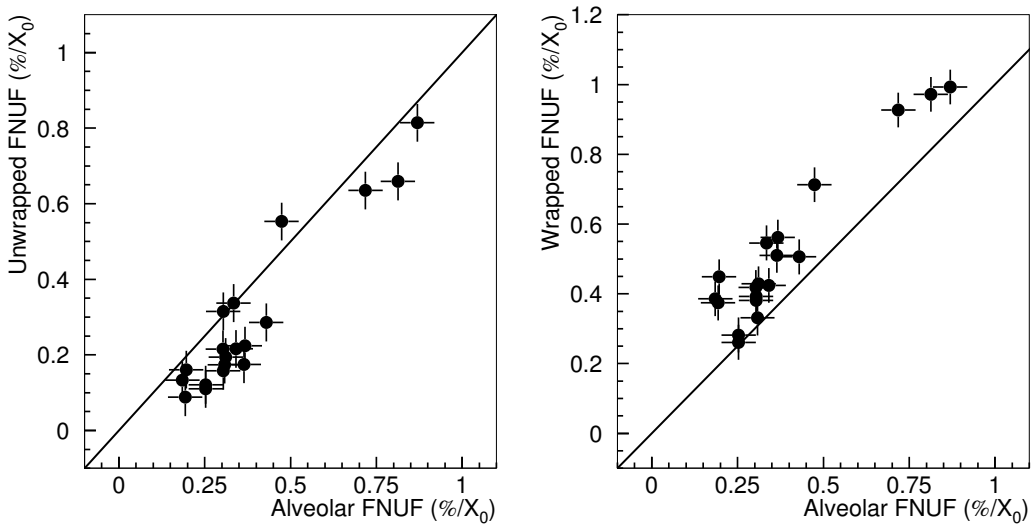

Fig. 7. Correlations between unwrapped FNUFs and wrapped and alveolar FNUFs. The diagonal lines represent the 1:1 correlation line.

second photon in the $PbWO_4$ crystal stops the measurement. This technique provides a relative value of light yield between each point. To obtain absolute light yields, the data are normalised to measurements made on wrapped crystals using a HPMT.

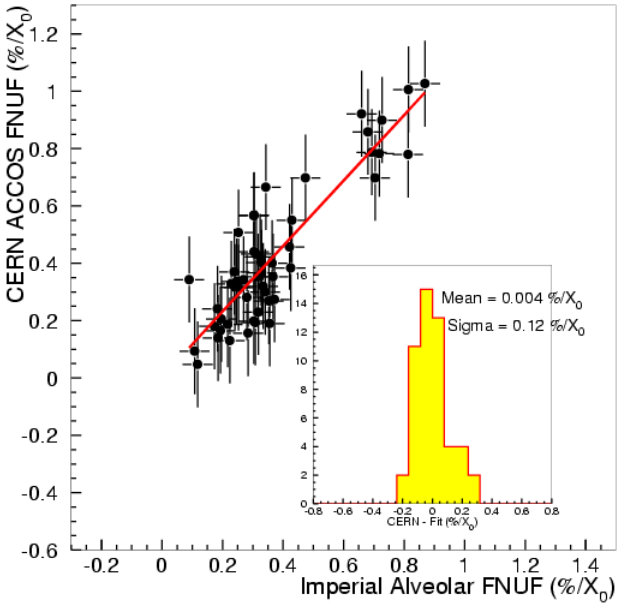

Fig. 8. The correlation between CERN ACCOS FNUFs and IC alveolar FNUFs. The inset histogram is the distribution of CERN data around the fitted correlation line (with the Imperial resolution subtracted in quadrature).

	Average FNUF ($\%/X_0$)	Average Light Yield* (N_{pe}/MeV)
ACCOS (20 crystals)	0.43 ± 0.03	11.0
Imperial Wrapped (20 crystals)	0.50 ± 0.01	11.21 ± 0.02
Imperial Alveolar (20 crystals)	0.38 ± 0.01	8.54 ± 0.02
ACCOS (51 crystals)	0.42 ± 0.02	10.9
Imperial Alveolar (51 crystals)	0.366 ± 0.007	8.99 ± 0.01

* No correction is applied to account for the different photocathode quantum efficiencies between the ACCOS PMT and the Imperial HPMT .

Table 2
Comparison of ACCOS and Imperial College measurements.

There is a clear correlation between the CERN ACCOS data and Imperial College data, as shown in Figure 8. From this correlation the precision of the ACCOS FNUF measurements has been estimated as $0.12\%/X_0$ which is consistent with a recently stated value of $0.15\%/X_0$ [8].

The average ACCOS FNUF is 0.05 $\%/X_0$ larger than our average alveolar FNUF and 0.07 $\%/X_0$ smaller than our wrapped data. These differences are

somewhat significant (at around the 3σ level) but perhaps could be explained by the different fitting procedures and the normalisation coefficients applied to the CERN data.

6 Crystal Chamfers

The CMS crystals have chamfered edges (as specified in Figure 9) to relieve stresses on the polished faces. Chamfers are produced by lapping the edges with a 15 μm diamond slurry [10] and represent about 2% of the total crystal surface area. Light that is normally retained by total internal reflection can escape through the chamfers, an effect which is enhanced due to the large number of reflections that a photon undergoes before being detected. Simulations have shown that the chamfers can have a noticeable effect on the crystal light collection uniformity [11]. Two methods of manipulating the chamfers

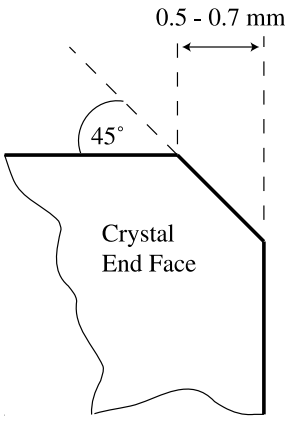

Fig. 9. Design specification of crystal chamfers.

to achieve the desired uniformity have been investigated. The first was to shade the chamfers using a HB pencil and the second involved de-polishing the chamfers. These two procedures are further described below.

7 Graphite Shading

7.1 Optimum Shading Length

Two reference crystals were measured in an alveolar with a tyvek endpiece at the tapered end. Shading was applied to all four chamfers in 1 cm steps using a HB pencil until the area was visibly coloured. The FNUF after each step was measured and the reduction in light yield was noted, as shown in Figure 10.

The FNUF appears to be reduced after shading has been applied, but no further reduction is apparent after the first few centimetres have been shaded. However, as the shading is extended the amount of light detected continues to decrease as more is absorbed. The optimum shading length seems to be about 6 cm as this is where the reduction in FNUF appears to have saturated but the amount of light lost is still small.

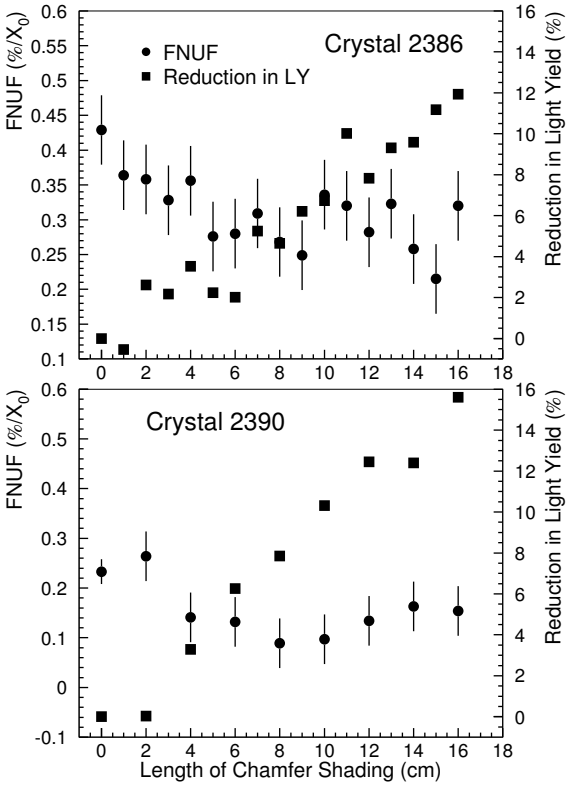

Fig. 10. FNUFs for 2 crystals measured as a function of shaded chamfer length. The percentage reduction in light yield with shaded length is also shown.

The 6cm shading was applied to all 52 crystals which were then measured in the alveolar with a tyvek endpiece. The results are shown in Figure 11. Six crystals could not be fitted due to low light yield.

The average FNUF is found to be 0.28 $\%/X_0$ for crystals with 6 cm shading inside the alveolar. For the same crystals measured in an alveolar with no shading, the average FNUF is 0.37 $\%/X_0$. Thus the shading technique achieves a reduction in FNUF of 0.09 $\%/X_0$, a significant difference. The fraction of crystals above the 0.35 $\%/X_0$ limit after shading has been applied is 21% compared to 35% before shading. However, if the anomalous crystals are ignored the fraction above the limit after shading is only 5%.

The uniformisation technique seems to work on both normal and anomalous FNUF crystals. The associated average reduction in light yield when shading is applied is 4%. The correlation between the FNUFs of shaded and unshaded crystals is shown in Figure 12; it can be seen that there is a shift towards higher FNUF for unshaded crystals but there is no evidence that the shift depends on the absolute value of the FNUF.

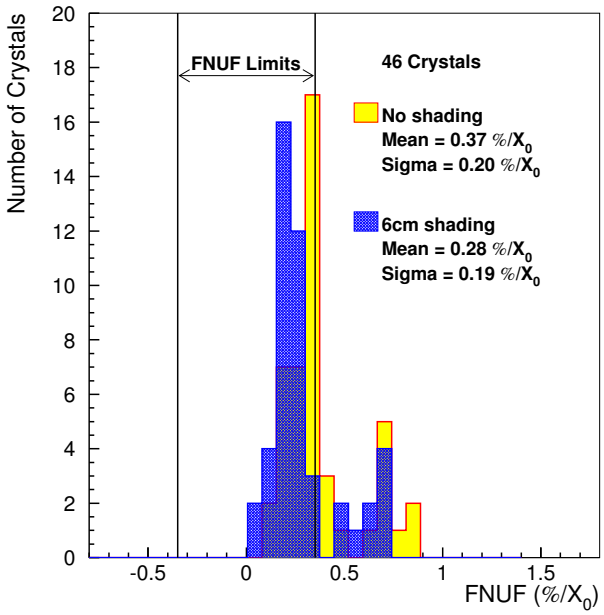

Fig. 11. Distribution of FNUFs before and after 6 cm shading has been applied.

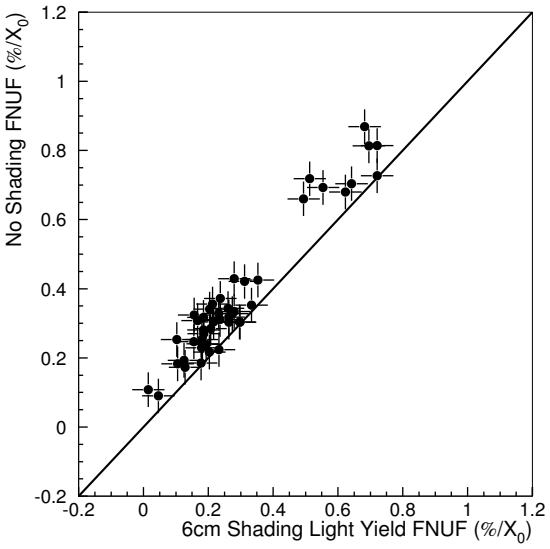

Fig. 12. Correlation between FNUFs for unshaded and shaded crystals.

7.2 Robustness of the Shading Technique

If the shading technique is to be employed on final production crystals for the detector then it must survive general handling during supercrystal assembly and detector construction.

A simple test was devised to investigate how robust the shading technique is. Two crystals were shaded and their FNUFs measured. The shaded areas of the chamfers were then wiped with a tissue and the crystals were remeasured. This was repeated several times. Figure 13 shows that for two crystals there appears to be no significant degradation of the shading effect even after many wipes. For the third crystal (2374), the FNUF starts to return to its unshaded value after two wipes. For all crystals the FNUF returned to the unshaded value after the graphite had been thoroughly cleaned off. We speculate that the reduction in FNUF is due to the graphite trapped in the roughened surface of the chamfer and does not result from the surface graphite which can easily be wiped off. It is possible that there is a wide variation in chamfer roughness from crystal to crystal; the smoother the chamfer the easier it is to wipe off the graphite.

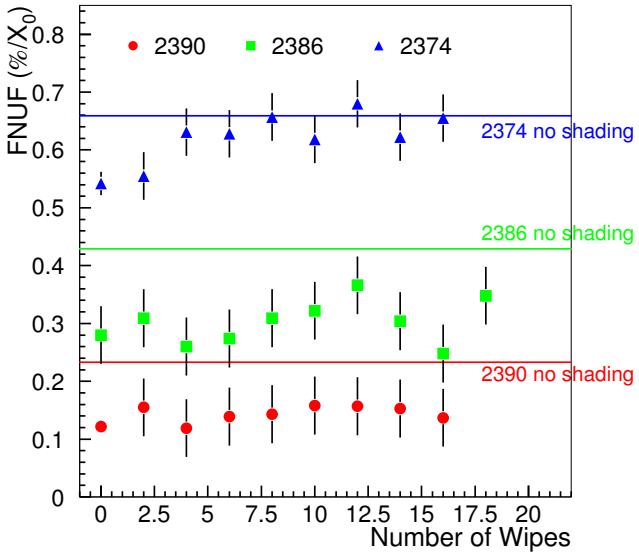

Fig. 13. FNUFs of shaded crystals after wiping with a tissue.

8 De-polishing Chamfers

In the section above, it was reported that reducing the FNUF can be achieved by shading the chamfers. The technique for uniformising barrel crystals involves de-polishing one of the long faces; it was speculated that the FNUF could be altered by changing the roughness of the lapping process used to machine the chamfers. It is not possible at this stage to alter the chamfer machining equipment at BTCP [10], but it was decided to test the idea by de-polishing the chamfers by hand.

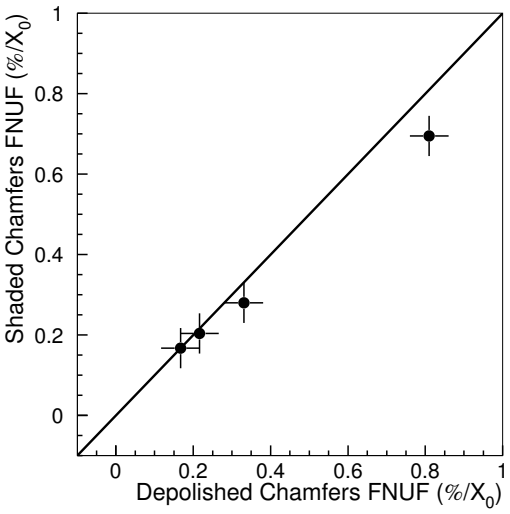

Fig. 14. The correlation between FNUFs for de-polished chamfers and 6cm-shaded chamfers.

The two faces adjacent to the chamfer being de-polished were first masked off to prevent damage. The crystal was submerged in water to prevent $PbWO_4$ dust being released into the immediate surroundings. Grade FF emery cloth was then used to roughen the entire length of the chamfer. No attempt was made to quantify the extent of roughening; the crystal was gently rubbed with the cloth until visibly roughened. This took approximately 3 - 4 minutes per chamfer.

8.1 Results

The technique described above has been applied to four crystals which had previously been measured in the alveolar un-shaded and with 6 cm shading. Although four crystals is not a large statistical sample, results are observed which are consistent with the results obtained for shaded crystals, namely an average reduction in FNUF of about 0.1 $\%/X_0$ and an average reduction in light yield of 4%. The correlation between shaded FNUFs and de-polished FNUFs is shown in Figure 14.

9 Conclusions

The non-uniformity of $PbWO_4$ endcap crystals can be measured with high precision using a HPMT. The effect of different crystal wrappings on the FNUF has been investigated. It was found that tyvek wrapping resulted in higher

FNUF when compared with unwrapped crystals or with crystals measured in the alveolar.

Studies of crystals in the alveolar have revealed that the average FNUF of 0.37 $\%/X_0$ is only slightly above the requirement of 0.35 $\%/X_0$ for the sample of crystals investigated. This leaves some hope that only mild uniformisation techniques will be required for a small subset of crystals failing to meet the specification.

The FNUF of 52 crystals for the CMS endcap electromagnetic calorimeter was reduced by an average of about 0.1 $\%/X_0$ when the four longitudinal chamfered edges were shaded with an ordinary lead pencil for about 6cm from the tapered end. Ignoring the anomalous FNUF crystals, this reduction in the average FNUF resulted in just 5% of the crystal sample remaining above the FNUF limit of 0.35 $\%/X_0$, compared to 21% before shading. The shading technique appears to be robust against handling and offers a simple method of applying mild uniformisation during the assembly to crystals that lie above the desired uniformity limit. A similar reduction in FNUF was observed on four crystals when the chamfers were roughened with emery paper. This offers the possibility of including the procedure in the manufacturing process in future projects.

References

[1] The CMS Collaboration, *"The Electromagnetic Calorimeter Project Technical Design Report"*, **CERN/LHCC 97-33**.

[2] D.J. Graham, C. Seez, *"Simulation of Longitudinal Light Collection Uniformity in $PbWO_4$ Crystals"*, **CMS Note 1996/002**.

[3] G.J. Davies *et al.*, *"Development of a Uniformisation Procedure for the $PbWO_4$ Crystals of the CMS Electromagnetic Calorimeter"*, **CMS Note 2001/004**.

[4] E. Auffray *et al.*, *"Performance of ACCOS, an Automatic Crystal Quality Control System for the PWO Crystals of the CMS Calorimeter"*, Nucl. Inst. Meth. **A456** (2001) p.325-341.

[5] D. Britton *et al.*, *"Precision fitting function for HPMT spectra"*, Nucl. Inst. Meth. **A504** (2003) p.298-300.

[6] E. Auffray, private communication.

[7] E. Auffray *et al.*, *"Evaluation of 100 Preproduction End Cap Crystals from BTCP"*, **CMS IN 2001/048**.

[8] E. Auffray *et al.*, *"Cross-calibration of two automatic quality control systems for the CMS ECAL crystals"*, **CMS Note 2003/003**.

[9] D. Britton *et al.*, *"Studies of $PbWO_4$ Endcap Crystals Using a Hybrid Photomultiplier Tube"*, CMS Note in preparation.

[10] Michel Lebeau, *Private communication.*

[11] D.I. Britton *et al.*, *" Simulation of the HPMT/VPT Light Collection Ratio"*, **CMS Note 2003/011**.